

See discussions, stats, and author profiles for this publication at: <https://www.researchgate.net/publication/255819135>

Conjugated and Nonconjugated Substitution Effect on Photovoltaic Properties of Benzodifuran-Based Photovoltaic Polymers

ARTICLE in MACROMOLECULES · SEPTEMBER 2012

Impact Factor: 5.8 · DOI: 10.1021/Ma301254x

CITATIONS

74

READS

37

8 AUTHORS, INCLUDING:



Lijun Huo

Beihang University(BUAA)

56 PUBLICATIONS 3,935 CITATIONS

[SEE PROFILE](#)



Long Ye

North Carolina State University

52 PUBLICATIONS 1,446 CITATIONS

[SEE PROFILE](#)



Xia Guo

Soochow University (PRC)

71 PUBLICATIONS 3,820 CITATIONS

[SEE PROFILE](#)



Maojie Zhang

Soochow University (PRC)

64 PUBLICATIONS 2,438 CITATIONS

[SEE PROFILE](#)

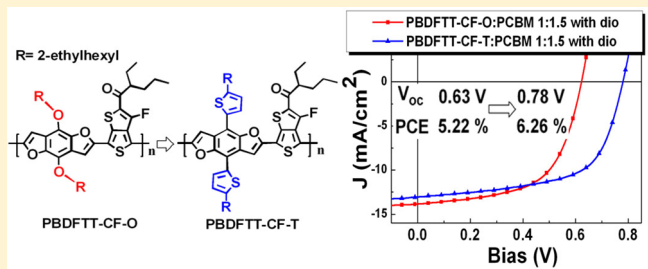
Conjugated and Nonconjugated Substitution Effect on Photovoltaic Properties of Benzodifuran-Based Photovoltaic Polymers

Lijun Huo, Long Ye, Yue Wu, Zhaojun Li, Xia Guo, Maojie Zhang, Shaoqing Zhang, and Jianhui Hou*

State Key Laboratory of Polymer Physics and Chemistry, Beijing National Laboratory for Molecular Sciences, Institute of Chemistry, Chinese Academy of Sciences, Beijing 100190, China

S Supporting Information

ABSTRACT: In order to investigate the influence of two-dimensional (2D) conjugated structure on photovoltaic properties of benzo[1,2-*b*:4,5-*b'*]difuran (BDF)-based polymers, two low band gap photovoltaic polymers, named PBDFTT-CF-O and PBDFTT-CF-T, were designed and synthesized. These two polymers have the same backbones and different side groups. Although these two polymers show similar optical band gaps (ca. 1.5 eV), the polymer with alkylthienyl side groups, PBDFTT-CF-T, exhibits stronger absorption in long wavelength direction than the polymer with alkoxy side groups, PBDFTT-CF-O. Meanwhile, PBDFTT-CF-T exhibits a HOMO level of -5.21 eV, which is 0.23 eV lower than that of PBDFTT-CF-O due to weaker electron-donating ability of alkylthienyl side groups than that of alkoxy side groups. The hole mobility of the blend of PBDFTT-CF-T/PC₇₁BM (1:1.5, w/w) is 0.128 cm² V⁻¹ s⁻¹, which is 1 order of magnitude higher than that of the blend of PBDFTT-CF-O/PC₇₁BM. Density functional theory (DFT) model shows thiophene pendants on dithienyl-BDF are more coplanar than it on dithienyl-BDT. These results indicate that the 2D-conjugated structure is helpful for molecular structure design of the BDF-based polymers in enhancing the intermolecular π - π stacking and improving charge transport property. Furthermore, the photovoltaic devices based on these two polymers show similar short circuit density and fill factor values, while the open circuit voltage of the PBDFTT-CF-T-based device is 0.78 V, which is 0.15 V higher than that of the PBDFTT-CF-O-based device. Therefore, the efficiencies of the devices based PBDFTT-CF-T/PC₇₁BM and PBDFTT-CF-O/PC₇₁BM are 6.26% and 5.22%, respectively. The results in this work demonstrate that the weak electron-donating ability of alkylthienyl side groups can be seen as an effective strategy to improve photovoltaic properties of the BDF-based polymers and the 2D-conjugated molecular structure is favorable to improve hole mobility.



INTRODUCTION

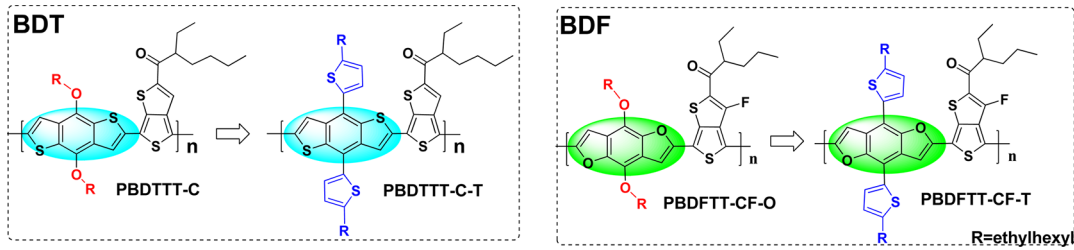
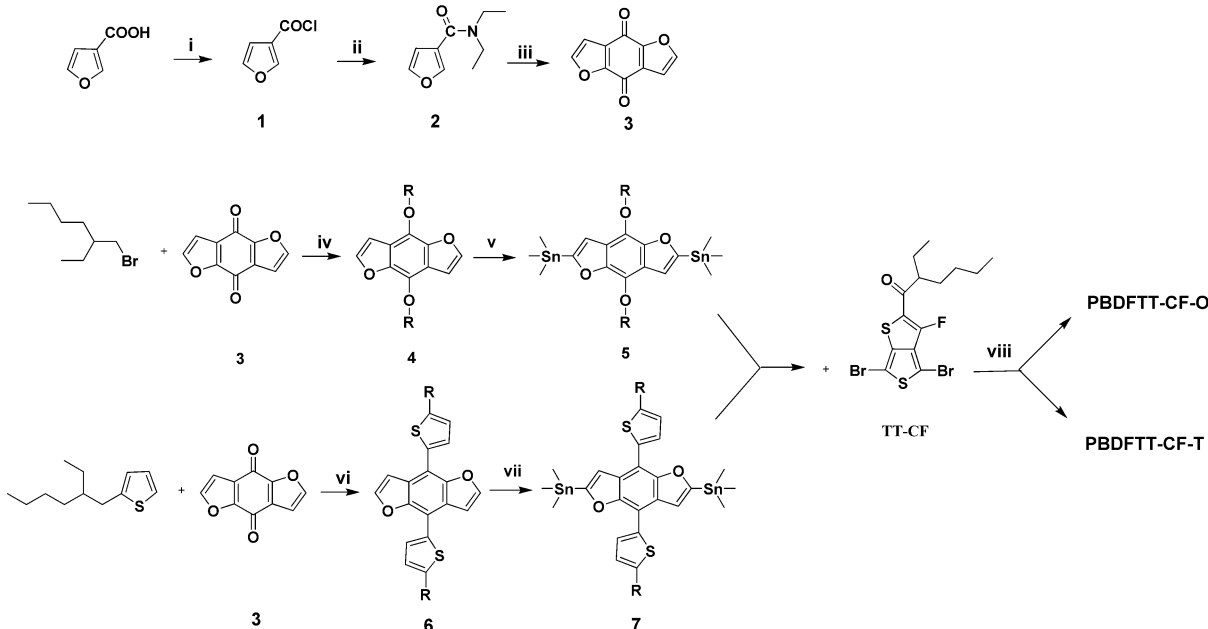
Polymer solar cells (PSCs) have made great progress in recent years.¹ Up to now, several groups have developed some highly efficient photovoltaic polymers, which showed promising power conversion efficiencies (PCEs) of 7–9% in bulk heterojunction cells devices.² The optimization of molecular structure of photovoltaic polymers is of great importance to realize high photovoltaic performance. It has been well-recognized that band gap, molecular energy level, and mobility are three key parameters for photovoltaic polymers. Different strategies have been developed to optimize those three parameters by modifying molecular structures of photovoltaic polymers. For example, band gaps of conjugated polymers can be reduced effectively by introducing D–A structure or quinoid structure; molecular energy levels of conjugated polymers can be tuned by introducing electron-rich/deficient building blocks or substituents; mobilities of conjugated polymers can be improved by increasing regularity of the backbone units.³ Beside those strategies listed as above, there are still a lot of successful examples for molecular structure optimization of photovoltaic polymers.⁴

To find a method to simultaneously obtain narrower band gap, a deeper HOMO level as well as higher mobility in one conjugated polymer is crucial to the study of photovoltaic polymers. Recently, our groups introduced two-dimensional (2D) conjugated structure to benzodithiophene (BDT)-based polymers,^{2a} and this kind of polymer shows similar band gaps, slightly deeper HOMO levels, higher mobilities, and hence better photovoltaic properties than the analogues without the 2D-conjugated structure. (see Scheme 1) Although the introduction of the 2D-conjugated structure has proven to be helpful in improving photovoltaic properties of BDT-based polymers, how this concept functions in other polymer systems is still unknown. Therefore, it is still necessary to do further investigation on the influence of 2D-conjugated structure on photovoltaic properties of different polymer systems.

In the field of organic semiconductors, furan and its derivatives attracted much less attention compared to thiophene-based heteroaromatic units. However, since furan-

Received: June 20, 2012

Revised: August 8, 2012

Scheme 1. Molecular Structures of the BDT-Based and BDF-Based Polymers**Scheme 2.** Synthetic Routes of PBDFTT-CF-O and PBDFTT-CF-T^a

^aReagents and conditions: (i) oxalyl chloride, room temperature, 12 h; (ii) diethylamine, methylene chloride, room temperature, 1 h; (iii) 0 °C, THF, *n*-butyllithium, then room temperature, 18 h, then HCl; (iv) 0 °C, ethanol, sodium borohydride, 3 h, HCl; then 2-ethylhexyl bromide, 150 °C, 15 h; (v) THF, *n*-butyllithium, room temperature, 1 h, then chlorotrimethylstannane, 30 min; (vi) *n*-butyllithium, THF, 0 °C, then 50 °C, 2 h; benzo[1,2-*b*:4,5-*b*']difuran-4,8-dione, 50 °C, 1 h, then SnCl₂, HCl; (vii) 0 °C, THF, *n*-butyllithium, then room temperature, 2 h, then chlorotrimethylstannane, 1 h; (viii) toluene/DMF, Pd(PPh₃)₄, 110 °C, 16 h.

based conjugated polymers exhibit some interesting properties, like planar molecular configuration,⁵ high solubility,⁶ and biodegradable and biorenewable properties,⁷ several conjugated polymers were developed and showed promising properties in optoelectronic devices in recent years.⁸ Our group previously designed and synthesized a conjugated polymer based on alkoxy-substituted benzo[1,2-*b*:4,5-*b*']difuran (BDF) and 4,7-dithienyl-2,1,3-benzothiadiazole (DTBT), named PBDF-DTBT,⁹ which showed promising photovoltaic properties. In this work, in order to develop new photovoltaic polymers based on BDF unit and investigate the influence of 2D-conjugated structure on photovoltaic properties of the BDF polymer, we tried to build a new polymer backbone based on BDF and thieno[3,4-*b*]thiophene (TT) and then apply the 2D-conjugated structure to this backbone, and hereby a new polymer, named PBDFTT-CF-T in Scheme 1, was designed. As a reference material, another new polymer based on alkoxy-substituted BDF, named PBDFTT-CF-O in Scheme 1, was also prepared and characterized in parallel with PBDFTT-CF-T.

EXPERIMENTAL SECTION

Materials. 4,8-Dehydrobenzo[1,2-*b*:4,5-*b*']dithiophene-4,8-dione (3), 4,8-bis(2-ethylhexyloxy)benzo[1,2-*b*;3,4-*b*]difuran (4), and 2,6-bis(trimethyltin)-4,8-bis(2-ethylhexyloxy)benzo[1,2-*b*:4,5-*b*']difuran (5) were prepared according to our modified method.⁹ 1-(4,6-Dibromo-3-fluorothieno[3,4-*b*]thiophen-2-yl)-2-ethylhexan-1-one (TT-CF) and 2-(2-ethylhexyl)thiophene were purchased from Solarmer Materials Inc.; Pd(PPh₃)₄ was purchased from Frontiers Scientific Inc. All of these chemicals were used as received. Tetrahydrofuran (THF) was dried over Na/benzophenone ketyl and freshly distilled prior to use. The other materials were commercial level and used as received.

Instruments. ¹H spectra were measured on a Bruker arx-400 spectrometer in CDCl₃ at 293 K. Absorption spectra were taken on a Hitachi U-3100 UV-vis spectrophotometer. The molecular weights of the polymers were measured by the GPC method, wherein polystyrene was used as a standard by using chloroform as eluent. TGA measurements were performed on a TA Instruments, Inc., TGA-2050. The electrochemical cyclic voltammetry (CV) was conducted on a CHI650D electrochemical workstation with Pt disk, Pt plate, and Ag/Ag⁺ electrode as working electrode, counter electrode, and reference electrode, respectively, in a 0.1 M tetrabutylammonium hexafluorophosphate (Bu₄NPF₆)—acetonitrile solution. Atomic force microscopy (AFM) measurement of the surface morphology of

samples was conducted on a Nanoscope III (Vecco) in tapping mode with a 2 μm scanner. Transmission electron microscopy (TEM) was performed using a JEOL 2200FS instrument at 160 kV accelerating voltage. The samples for the TEM measurements were prepared as follows: the thin active-layer (about 100 nm) films were spin-cast on ITO/PEDOT:PSS substrates, and the ITO glass with the active layers was submerged in deionized water to make the active layers floated onto the air/water interface. Then the floated films were picked up on unsupported 200 mesh copper grids for the TEM measurement. The external quantum efficiency (EQE) was measured by an Enli Technology solar cell spectral response measurement system (QE-R3011). The light intensity at each wavelength was calibrated with a standard single-crystal Si photovoltaic cell.

Hole Mobility Measurement. We used a device structure of ITO/PEDOT:PSS/polymers:PC₇₁BM/Au for the hole mobility measurement, based on the space-charge-limited current (SCLC) model. According to the following equation: $\ln(JL^3/V^2) \approx 0.89(1/E_0)^{0.5}(V/L)^{0.5} + \ln(9\varepsilon\varepsilon_0\mu_0/8)$, where μ_0 is the zero-field mobility, E_0 is the characteristic field, J is the current density, ε is the dielectric constant of the polymer, ε_0 is the permittivity of the vacuum, L is the thickness of the polymer layer, $V = V_{\text{appl}} - V_{\text{bi}}$, V_{appl} is the applied potential, and V_{bi} is the built-in potential (in this device structure, $V_{\text{bi}} = 0.2$ V). According to the equation, hole mobility can be calculated.

Fabrication of Polymer Solar Cells. Polymer solar cell devices were fabricated under conditions as follows: After spin-coating a 35 nm layer of poly(3,4-ethylenedioxythiophene):poly(styrenesulfonate) (PEDOT:PSS) onto a precleaned indium–tin oxide (ITO)-coated glass substrates, the polymer/PC₇₁BM blend solution was spin-coated. The concentration of the polymer:PC₇₁BM blend solutions used in this study for spin-coating was 10 mg/mL (polymer/*o*-dichlorobenzene), and *o*-dichlorobenzene was used as the solvent. The additive, 1,8-diiodooctane (DIO) with 3% volume ratio was added prior to the spin-coating process. The thickness of the active layer was controlled by changing the spin speed during the spin-coating process and measured on an Ambios Tech. XP-2 profilometer. The devices were completed by evaporating Ca/Al metal electrodes with an effective area of 4 mm² as defined by masks. The current–voltage curves were measured under 100 mW cm⁻² standard AM 1.5 G spectrum using a XES-70S1 (San-EI Electric Co., Ltd.) solar simulator (AAA grade, 70 mm × 70 mm photobeam size). Two cm × 2 cm monocrystalline silicon reference cell (SRC-1000-TC-QZ) was purchased from VLSI Standards Inc.

Synthesis. The synthetic routes of the monomers and polymers are shown in Scheme 2. The detailed synthetic processes are as follows.

4,8-Bis(5-(2-ethylhexyl)thiophen-2-yl)benzo[1,2-*b*:4,5-*b'*]difuran (6). In a 100 mL argon purged flask, *n*-butyllithium (2.5 M, 3.52 mL) was added into a solution of 2-(2-ethylhexyl)thiophene (1.57 g, 8 mmol) in THF (30 mL) dropwise at 0 °C; then the mixture was warmed up to 50 °C and stirred for 1 h. Subsequently, 4,8-dehydrobenzo[1,2-*b*:4,5-*b'*]difuran-4,8-dione (0.38 g, 2 mmol) was added, and the mixture was stirred for 1 h at 50 °C. After cooling down to ambient temperature, a mixture of SnCl₂·2H₂O (4.5 g, 20 mmol) in 10% HCl (8 mL) was added, and the mixture was stirred for an additional 1.5 h and then poured into ice water. The mixture was extracted by ethyl ether twice, and the combined organic phase was concentrated to obtain the raw compound 6. Further purification was carried out by a silica gel column using petroleum ether as eluent to obtain pure compound 6 as a pale yellow sticky liquid (0.48 g, yield 44%). ¹H NMR (CDCl₃, 400 MHz), δ (ppm): 7.77 (d, 2H), 7.68 (d, 2H), 7.37 (d, 2H), 6.89 (d, 2H), 2.85 (d, 4H), 1.70 (m, 2H), 1.463–1.25 (br, 16H), 0.95–0.91 (m, 12H). ¹³C NMR (CDCl₃, 100 MHz), δ (ppm): 148.87, 145.72, 145.28, 134.36, 127.78, 125.89, 123.43, 110.34, 107.36, 41.71, 34.38, 32.68, 29.14, 25.83, 23.26, 14.38, 11.09. Elements analysis: calcd: C, 74.68; H, 7.74; found: C, 74.65; H, 7.73.

2,6-Bis(trimethyltin)-4,8-bis(5-(2-ethylhexyl)thiophen-2-yl)benzo[1,2-*b*:4,5-*b'*]difuran (7). In a 50 mL argon-purged flask, *n*-butyllithium (2.5 M, 0.48 mL) was added into a solution of compound 6 (0.22 g, 0.4 mmol) in THF (20 mL) at 0 °C; then the mixture was stirred for 2 h at ambient temperature. Subsequently, chlorotrimethyl-

stannane (1.0 M in hexane, 2 mL) was added, and the mixture was stirred for 1 h at ambient temperature. Then the mixture was extracted by ethyl ether, and the combined organic phase was concentrated to obtain compound 7. Further purification was carried out by recrystallization using ethanol as solvent to obtain pure compound 7 as light yellow solid (0.27 g, yield 77%). ¹H NMR (CDCl₃, 400 MHz), δ (ppm): 7.72 (d, 2H), 7.50 (s, 2H), 6.90 (d, 2H), 2.88 (d, 4H), 1.74 (m, 2H), 1.54–1.33 (br, 16H), 0.95 (m, 12H), 0.47 (s, 18H). ¹³C NMR (CDCl₃, 100 MHz), δ (ppm): 166.26, 152.37, 144.64, 135.52, 127.19, 125.68, 123.51, 117.97, 108.64, 41.64, 34.30, 32.65, 29.14, 25.80, 23.23, 14.36, 11.10, –8.79. Elements analysis: calcd: C, 55.07; H, 6.70; found: C, 55.11; H, 6.71.

General Method of Polymerization by Stille Coupling Reaction for the Polymers.

Compound 5 or compound 7 (0.5 mmol) and TT-CF (0.5 mmol) were mixed in 10 mL of toluene and 2 mL of DMF. After being purged by argon for 5 min, 30 mg of Pd(PPh₃)₄ was added as catalyst, and then the mixture was purged by argon for 25 min. The reactant was stirred and heated to reflux for 16 h. Then the reactant was cooled to room temperature, and the polymer was precipitated by addition of 50 mL of methanol, and then filtered through a Soxhlet thimble, which was then subjected to Soxhlet extraction with methanol, hexane, and chloroform. The polymer was recovered as solid from the chloroform fraction by precipitation from methanol. The solid powders were dried under vacuum. The yields and molecular weight results of the polymers are as follows: PBDFTT-CF-O: yield: 56%. Elements analysis: calcd: C, 69.13; H, 7.40; found: C, 69.22; H, 7.33. $M_w = 14K$, PDI = 3.0. PBDFTT-CF-T: yield: 47%. Elements analysis: calcd: C, 69.69; H, 6.70; found: C, 69.48; H, 6.78. $M_w = 17K$, PDI = 3.6.

RESULTS AND DISCUSSION

Synthesis and Structural Characterization. The synthetic routes of PBDFTT-CF-O and PBDFTT-CF-T are shown in Scheme 2. Pure 4,8-dehydrobenzo[1,2-*b*:4,5-*b'*]dithiophene-4,8-dione (3) can be obtained from several recrystallizations in acetic acid. 4,8-Bis(2-ethylhexyloxy)benzo[1,2-*b*:4,5-*b'*]difuran (4) and 2,6-bis(trimethyltin)-4,8-bis(2-ethylhexyloxy)benzo[1,2-*b*:4,5-*b'*]difuran (5) were prepared according to modified our previous work.⁹ The 2D-conjugated BDF monomer was synthesized easily through two steps. Under 0 °C, *n*-butyllithium was added to 2-ethylhexylthiophene to form (5-(2-ethylhexyl)thiophen-2-yl)lithium, and then benzo[1,2-*b*:4,5-*b'*]difuran-4,8-dione was added at 50 °C and the reactant was stirred under 50 °C for 2 h, and then a solution of SnCl₂ in hydrochloric acid was added. Compound 6 can be purified by silica gel column using petroleum ether as eluent and obtained in a yield of 44%. Subsequently, compound 7 was prepared with a yield of 77% through the same method as used in the synthesis of 2D-conjugated BDT monomer.^{2a} These two polymers were prepared by Stille coupling reactions, and the yields are 56% and 47% for PBDFTT-CF-O and PBDFTT-CF-T, respectively. Both of these two polymers show excellent solubility in tetrahydrofuran, chloroform, toluene, dichlorobenzene, etc. Although different methods were tried to increase the polymerization degree, the molecular weights of the polymers are still lower than the majority of the conjugated polymers used in photovoltaic applications. The molecular weights of these two polymers were estimated by the gel permeation chromatography (GPC) method using chloroform as eluent and monodispersed polystyrene as standard. For PBDFTT-CF-O and PBDFTT-CF-T, the weight-average molecular weights (M_w) are 14K and 17K, and the polydispersity index (PDI) are 3.0 and 3.6, respectively. Compared to other conjugated polymers, these two new BDF-based polymers show lower molecular weight values, and higher molecular weight products

can be expected if microwave condition can be used in the Stille polycondensation reaction.¹⁰

Optical Properties. The photophysical characteristics of the polymers were investigated by ultraviolet–visible (UV–vis) absorption spectroscopy in dilute chloroform solutions and as spin-coated films on quartz substrates. The absorption spectra of PBDFTT-CF-O and PBDFTT-CF-T in solution and as solid films are shown in Figure 1. According to the absorption

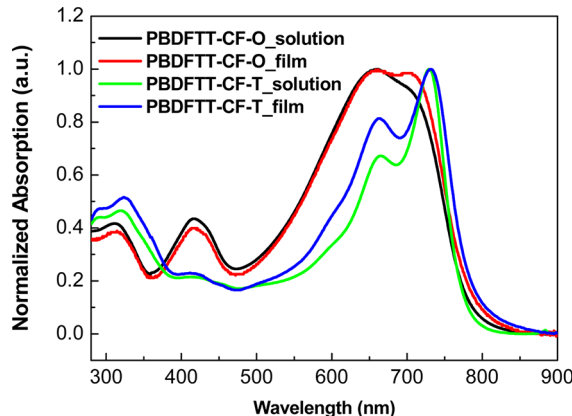


Figure 1. Absorption spectra of PBDFTT-CF-O and PBDFTT-CF-T in chloroform solutions and in solid films on quartz.

spectra of the films, the optical band gaps (E_g^{opt}) of PBDFTT-CF-O and PBDFTT-CF-T are 1.51 and 1.49 eV, respectively. Although the optical band gaps of these two polymers are quite similar, PBDFTT-CF-T shows much narrower absorption peak than PBDFTT-CF-O. In the visible range of 400–700 nm, PBDFTT-CF-T shows the weaker absorption intensity compared to that of PBDFTT-CF-O, indicating the $\pi-\pi^*$ transition of PBDFTT-CF-T are located at the low-energy region mainly, and thus the π -electrons of PBDFTT-CF-T might be delocalized better than the π -electrons of PBDFTT-CF-T. The solution and the film of PBDFTT-CF-T show two absorption peaks at 660 and 706 nm. The absorption peak located at 660 nm is ascribed to the intramolecular $\pi-\pi^*$ transition of the backbones, indicating that the two polymers should have similar effective conjugated length, and therefore the replacement of alkoxy groups by alkylthienyl groups has little influence on the conformation of the backbone units in these two polymers; i.e., the dihedral angels between the adjacent backbone units in these two polymers should be much similar. The absorption peak at 706 nm is ascribed to the intermolecular $\pi-\pi^*$ transition. Compared to PBDFTT-CF-O, PBDFTT-CF-T shows much stronger absorption in long wavelength direction, implying that the intermolecular $\pi-\pi^*$ transition in PBDFTT-CF-T is much stronger than that in PBDFTT-CF-O, and thus the introduction of 2D-conjugated structure might be helpful to enhance intermolecular $\pi-\pi$ stacking of the polymer.

Electrochemical Properties. Electrochemical cyclic voltammetry (CV) was employed to measure the polymers' oxidation/reduction onset potentials. From Figure 2, it can be seen that p-doping processes of both PBDFTT-CF-O and PBDFTT-CF-T are reversible. The oxidation onset potentials of PBDFTT-CF-O and PBDFTT-CF-T are 0.18 and 0.41 V, respectively. In the reduction processes, both two polymers exhibit similar reduction onset values at ca. -1.6 eV. The HOMO/LUMO levels of the polymers can be calculated

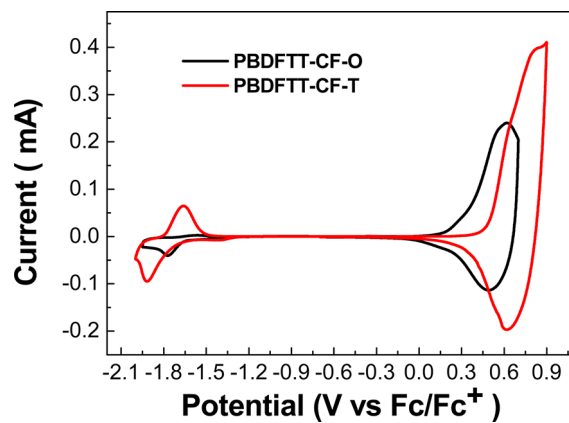


Figure 2. Cyclic voltammograms of PBDFTT-CF-O and PBDFTT-CF-T films on a platinum electrode in acetonitrile solution containing 0.1 M Bu_4NPF_6 at a scan rate of 20 mV/s.

according to the following equations: $E_{\text{LUMO}} = -e(E_{\text{red}} + 4.8)$ (eV) and $E_{\text{HOMO}} = -e(E_{\text{ox}} + 4.8)$ (eV), where the units of E_{ox} and E_{red} are in V vs Fc/Fc⁺. The HOMO and LUMO levels of PBDFTT-CF-O and PBDFTT-CF-T are -4.98 eV/-3.18 eV and -5.21 eV/-3.20 eV, respectively. It is obvious that the HOMO level of PBDFTT-CF-T is 0.23 eV lower than that of PBDFTT-CF-O, implying that the weak electron-donating ability of alkylthienyl side groups is favorable to lowering the HOMO level of the polymer, and hence the PSC device based on PBDFTT-CF-T may possess higher open-circuit voltage (V_{oC}) than that of PBDFTT-CF-O-based PSC device.^{2a} As reported in our previous work in Table 1, in the polymer

Table 1. Electrochemical Data, Molecular Energy Levels and Optical Band Gaps Comparisons among PBDFTT-CF-O, PBDFTT-CF-T, PBDTTT-C, and PBDTTT-C-T

	$E_{\text{onset}}^{\text{ox}}$ (V)	$E_{\text{onset}}^{\text{red}}$ (V)	HOMO (eV)	LUMO (eV)	$E_g^{\text{opt} \text{a}}$ (eV)	$E_g^{\text{ec} \text{b}}$ (eV)
PBDFTT-CF-O	0.18	-1.62	-4.98	-3.18	1.51	1.80
PBDFTT-CF-T	0.41	-1.60	-5.21	-3.20	1.49	2.01
PBDTTT-C ^c	0.27	-1.59	-5.07	-3.21	1.60	1.86
PBDTTT-C-T ^c	0.31	-1.55	-5.11	-3.25	1.58	1.86

^a $E_g^{\text{opt}} = \lambda_{\text{abs},\text{onset}}/1240$. ^bCalculated from $E_g^{\text{ec}} = e(E_{\text{onset}}^{\text{ox}} - E_{\text{onset}}^{\text{red}})$.

^cReference 2a.

system based on BDT and TT, HOMO levels of the polymers can be slightly reduced by replacing alkoxy groups with alkylthienyl groups; i.e., the HOMO level of PBDTTT-C-T is 0.04 eV lower than that of PBDTTT-C-O. It is obviously that the alkylthienyl side groups exhibit stronger effect on lowering HOMO level of the BDF-based polymer than on BDT-based polymer.

Quantum chemistry calculation by the DFT (B3LYP/6-31G** level) method was employed to demonstrate the electronic structures of these polymers. To simplify the calculations, long alkyl side chains were replaced by methyl. From simulated models in Table 2, we found that the LUMO orbitals of these four polymers are localized at the TT units mainly, while their HOMO orbitals are distributed along the whole molecules. Moreover, two phenomena should be noted. First, for PBDFTT-CF-T and PBDTTT-C-T, the wave functions of their HOMO levels can be delocalized onto the alkylthienyl groups, indicating that the π -electrons can be delocalized better by introducing the 2-D conjugated structure.

Table 2. Optimized Geometries and Molecular Orbital Surfaces of the HOMO and LUMO of the Model Compounds, Obtained at the DFT/B3LYP/6-31G* Level

Polymer	Structure	θ (degree)	HOMO orbit	LUMO orbit
PBDFTT-CF-O		--		
PBDFTT-CF-T		31		
PBDTTT-C		--		
PBDTTT-C-T		53		

Second, since the diameter of oxygen atom is much smaller than that of sulfur atom, compared to BDT unit, BDF unit exhibits smaller steric hindrance to the substituent on its 4- and 8-positions, and thus the torsion angle between the alkylthienyl group and the backbone unit in PBDFTT-CF-T is smaller than that in PBDTTT-C-T. Consequently, the wave function of the HOMO level of PBDFTT-CF-T can be delocalized to the alkylthienyl side groups more effectively than that of PBDTTT-CF-T.

Photovoltaic Properties. The PSC devices with a structure of ITO/PEDOT:PSS/polymers:PC₇₁BM/Ca/Al were fabricated to investigate photovoltaic properties of these two polymers. Both PBDFTT-CF-O/PC₇₁BM and PBDFTT-CF-T/PC₇₁BM blends were dissolved into *o*-dichlorobenzene to make the solutions of the D/A blends for spin-coating, and different weight ratios of polymer donor to PC₇₁BM were scanned. The current density–voltage (*J*–*V*) curves of the PBDFTT-CF-O/PC₇₁BM-based and PBDFTT-CF-T/PC₇₁BM-based PSC devices with optimum D/A ratios under the illumination of AM 1.5G (100 mW/cm²) are shown in Figure 3; the basic photovoltaic data for D/A ratio scan are listed in Table 3, and the photovoltaic results of the BDT analogues are included for making clear comparisons. The *V*_{oc}, the short-circuit current density (*J*_{sc}), and the fill factors (FF) of PBDFTT-CF-O/PC₇₁BM-based devices with different D/A ratios are 0.60–0.63 V, 9.76–12.59 mA/cm², and 47.1–59.7%, respectively. Correspondingly, the PCEs of the devices vary from 2.85% to 5.22%. From the device based on PBDFTT-CF-O/PC₇₁BM with a optimum D/A ratio (polymer:PC₇₁BM = 1:1.5), a PCE of 4.52% with *V*_{oc} = 0.63 V, *J*_{sc} = 12.51 mA/cm², FF = 0.57 was recorded. In order to further optimize photovoltaic performance, 3% (v/v) 1,8-diiodooctane (DIO) was used as additive in the solution of active layer materials.¹¹ We found that after adding DIO, the *J*_{sc} of the device can be improved slightly, from 12.51 to 13.87 mA/cm², and thus a PCE of 5.22% can be obtained. The optimum D/A ratio of PBDFTT-CF-T/PC₇₁BM system is 1:1.5, and after adding DIO as additive, photovoltaic performance of the device can be improved, from 4.54% to 6.26%, benefiting from the increase of

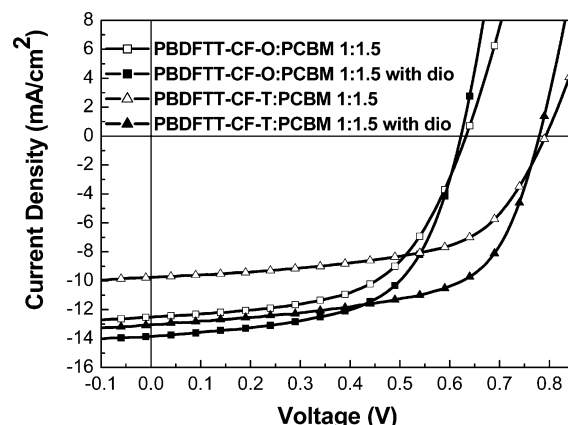


Figure 3. *J*–*V* curves of the PSCs based on PBDFTT-CF-O/PC₇₁BM and PBDFTT-CF-T/PC₇₁BM under the illumination of AM 1.5G, 100 mW/cm².

*J*_{sc}. According to the *J*–*V* curves, it is quite clear that the devices based on PBDFTT-CF-O and PBDFTT-CF-T fabricated through the optimum conditions show much similar *J*_{sc} and FF values, but *V*_{oc} of the PBDFTT-CF-T/PC₇₁BM-based devices is 0.15 V higher than that of the PBDFTT-CF-O/PC₇₁BM-based devices. Therefore, from PBDFTT-CF-O/PC₇₁BM to PBDFTT-CF-T/PC₇₁BM, PCE of the devices improved by 20%. Comparing the optimized photovoltaic results of the BDT-based analogues with these two BDF-based polymers (see the data in Table 3), the PCEs of the polymers can be improved by using the 2-D conjugated structure. Interestingly, from PBDTTT-C to PBDTTT-C-T, an improvement of 40 mV of *V*_{oc} was observed; however, from PBDFTT-CF-O to PBDFTT-CF-T, an improvement of 160 mV can be realized. The change of the *V*_{oc} values matches well with the results obtained from HOMO level (see Table 1), indicating that the 2-D conjugated structure has different influence on conjugated polymers with different backbone structures. From PBDFTT-CF-O to PBDFTT-CF-T, the distinguished improvement in HOMO level, and thus *V*_{oc} should be due to the reduced electron-donating effect caused by the side groups

Table 3. Photovoltaic Results of the PSCs Based on PBDFTT-CF-O/PC₇₁BM and PBDFTT-CF-T/PC₇₁BM under the Illumination of AM 1.5G 100 mW/cm²

polymers: PC ₇₁ BM	D/A ratio	film thickness (nm)	V _{oc} (V)	J _{sc} (mA/cm ²)	FF (%)	PCE (%)
PBDFTT-CF-O	1:1	100	0.62	9.76	47.14	2.85
	1:1.5	110	0.63	12.51	57.34	4.52
	1:1.5 ^a	114	0.63	13.87	59.70	5.22
	1:2	105	0.60	12.59	55.77	4.21
PBDFTT-CF-T	1:1	108	0.8	8.62	48.98	3.38
	1:1.5	105	0.79	9.79	58.76	4.54
	1:1.5 ^a	110	0.78	13.04	61.55	6.26
	1:2	95	0.78	9.00	59.8	4.20
PBDTTT-C ^b	1:1.5 ^a	120	0.70	15.51	59.2	6.43
PBDTTT-C-T ^b	1:1.5 ^a	140	0.74	17.48	58.7	7.59

^a3% v/v DIO was added. ^bOptimized results from ref 2a.

because the alkoxy should have a stronger electron-donating effect than the alkylthienyl group.

The external quantum efficiency (EQE) curves of the devices based on PBDFTT-CF-O/PC₇₁BM and PBDFTT-CF-T/PC₇₁BM (w/w, 1:1.5) prepared under optimum conditions are shown in Figure 4. Since the two devices shows similar EQE

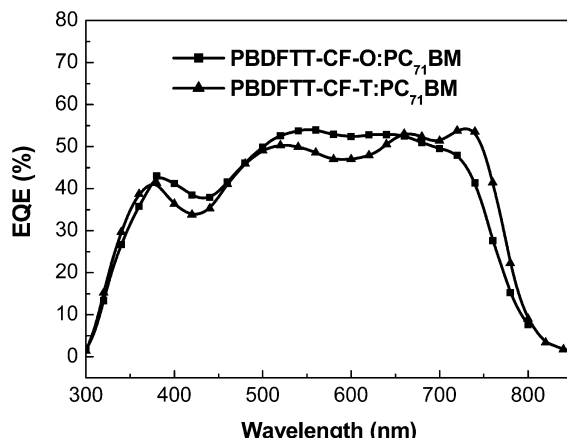


Figure 4. External quantum efficiency (EQE) curves of PBDFTT-CF-O- and PBDFTT-CF-T-based PSCs with a D/A ratio of 1:1.5 treated by using additive (DIO, 3% v/v).

in the whole response region, the integral current density values of the two devices deduced from the EQE curves and the standard solar spectrum are quite similar, which is coincident with we observed in J-V measurements. These two devices exhibit broad response in the visible light region, from 400 to 800 nm. The EQE peak values of these two devices reach over 50%. Considering that PBDFTT-CF-T/PC₇₁BM-based device shows a very broad response range, from 400 to 800 nm, if the EQE of the device can be improved to over 70%, the current density of the device would be increased tremendously, and theoretically, a J_{sc} of ~18 mA/cm² can be expected.

The hole mobility of the blend films of PBDFTT-CF-O/PC₇₁BM and PBDFTT-CF-T/PC₇₁BM (w/w, 1:1.5) prepared by the same conditions as used in fabricating the active layers of the champion PSC devices were measured by the space-charge-limited current (SCLC) method with a device structure of ITO/PEDOT:PSS/polymers:PC₇₁BM/Au. Interestingly, both two kinds of blends show rather high hole mobilities, 0.128 and 5.76 × 10⁻² cm² V⁻¹ s⁻¹ for PBDFTT-CF-T/PC₇₁BM and PBDFTT-CF-O/PC₇₁BM, respectively. Since the hole mobility of PBDFTT-CF-T/PC₇₁BM is more than 1 order of magnitude

higher than that of the blend film of PBDFTT-CF-O/PC₇₁BM, it can be concluded that the 2D conjugated structure is helpful to facilitate the charger transport of the polymer, benefiting from the extended conjugated area and hence the enhanced intermolecular π-π interaction. The above conclusion is also coincident with the reported results from 2-D conjugated BDT system.^{2a}

Surface morphology of the blend films of PBDFTT-CF-O/PC₇₁BM and PBDFTT-CF-T/PC₇₁BM with and without DIO were investigated by the atomic force microscope (AFM). As shown in Figures 5a and 5b, without adding DIO, the root-mean-square roughness (R_q) of the PBDFTT-CF-O/PC₇₁BM and PBDFTT-CF-T/PC₇₁BM films are 2.6 and 3.5 nm, respectively. However, when DIO was used as additive during the spin-coating process, R_q values of the blend films increased to 8.9 and 6.0 nm for the films of PBDFTT-CF-O/PC₇₁BM and PBDFTT-CF-T/PC₇₁BM, respectively. Transmission electron microscopy (TEM) was employed to further investigate the morphology of the blend films. The effects of DIO treatment on morphology of the blend films are well demonstrated as shown in Figure 5. As shown in Figures 5a and 5b, PBDFTT-CF-O/PC₇₁BM and PBDFTT-CF-T/PC₇₁BM exhibit very similar phase separation, wherein 100–350 nm dark domains are formed. Since PC₇₁BM has higher scattering density than the polymer, these dark domains should be ascribed to the aggregations of PC₇₁BM.¹² These large dimensions are much greater than the typical organic exciton diffusion length (ca. 10 nm as reported)¹³ and thereby limit device performance. Upon addition of 3% DIO, a significant reduction in phase separation is observed in Figures 5c and 5d. On the basis of the observations in the AFM and TEM images, it can be concluded that after adding DIO, the roughness of the blend films based on both two polymers increased slightly, while the phase separation of the blends reduced distinctly.

CONCLUSION

Two new low band gap conjugated polymers based on BDF were designed, synthesized, and applied in PSCs. In order to investigate the influence of 2D conjugated structure on photovoltaic properties of the BDF-based polymers, non-conjugated alkoxy and conjugated alkylthienyl are used as side groups in PBDFTT-CF-O and PBDFTT-CF-T, respectively. Compared to PBDFTT-CF-O, PBDFTT-CF-T shows stronger intermolecular π-π interaction in solution state and solid film, deeper HOMO level, and higher hole mobility. Under optimum device fabrication conditions, the PSC based on PBDFTT-CF-T/PC₇₁BM exhibits similar J_{sc} and FF but higher

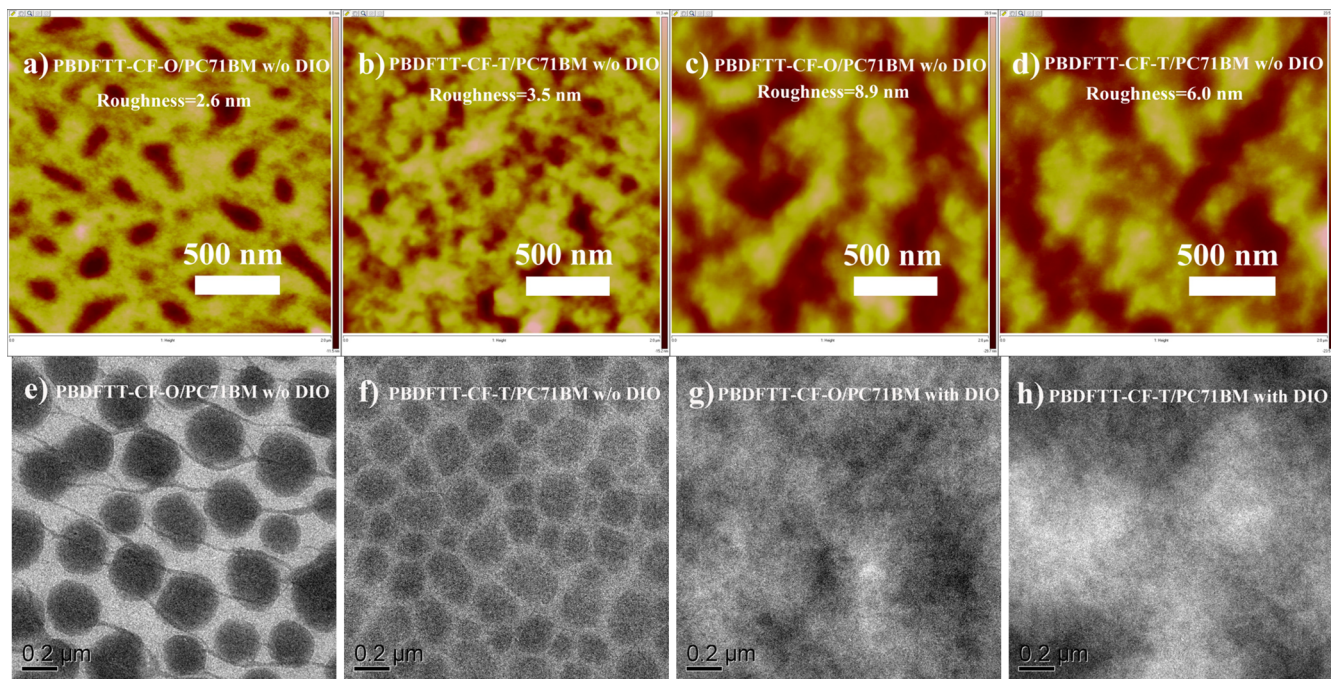


Figure 5. AFM height images ($2 \times 2 \mu\text{m}^2$) (a–d) and TEM images (e–h) of the blend films of PBDFTT-CF-O/PC₇₁BM and PBDFTT-CF-T/PC₇₁BM (1:1.5 w/w) prepared by different processes.

V_{oc} . Therefore, the efficiencies of the PSC devices based on PBDFTT-CF-T/PC₇₁BM and PBDFTT-CF-O/PC₇₁BM are 6.26% and 5.22%, respectively. The results in this work clearly demonstrate that BDF-based conjugated polymers are promising photovoltaic materials, and the 2D-conjugated structure can be seen as a simple but effective strategy to improve their photovoltaic properties.

ASSOCIATED CONTENT

Supporting Information

Experimental details. This material is available free of charge via the Internet at <http://pubs.acs.org>.

AUTHOR INFORMATION

Corresponding Author

*E-mail: hzhlz@iccas.ac.cn.

Notes

The authors declare no competing financial interest.

ACKNOWLEDGMENTS

This work was supported by National High-tech R&D Program of China (863 Program) (No. 2011AA050523) and National Natural Science Foundation of China (NSFC) (No. 21104088, 51173189).

REFERENCES

- (a) Chochos, C. L.; Chouliis, S. A. *Prog. Polym. Sci.* **2011**, *36*, 1362. (b) Cheng, Y.-J.; Yang, S.-H.; Hsu, C.-S. *Chem. Rev.* **2009**, *109*, 5868. (c) Thompson, B. C.; Fréchet, J. M. J. *Angew. Chem., Int. Ed.* **2008**, *47*, 58. (d) Chen, J. W.; Cao, Y. *Acc. Chem. Res.* **2009**, *42*, 1709. (e) Li, Y. F. *Acc. Chem. Res.* **2012**, *45*, 723.
- (a) Huo, L. J.; Zhang, S. Q.; Guo, X.; Xu, F.; Li, Y. F.; Hou, J. H. *Angew. Chem., Int. Ed.* **2011**, *50*, 9697. (b) Chen, H. Y.; Hou, J. H.; Zhang, S. Q.; Liang, Y. Y.; Yang, G. W.; Yang, Y.; Yu, L. P.; Wu, Y.; Li, G. *Nat. Photonics* **2009**, *3*, 649. (c) Price, S. C.; Stuart, A. C.; Yang, L.; Zhou, H.; You, W. *J. Am. Chem. Soc.* **2011**, *133*, 4625. (d) Chu, T.-Y.; Lu, J.; Beaupré, S.; Zhang, Y.; Pouliot, J.; Wakim, S.; Zhou, J.; Leclerc, M.; Li, Z.; Ding, J.; Tao, Y. *J. Am. Chem. Soc.* **2011**, *133*, 4250. (e) Zhou, H.; Yang, L.; Stuart, A. C.; Price, S. C.; Liu, S.; You, W. *Angew. Chem., Int. Ed.* **2011**, *50*, 2995. (f) Huang, Y.; Guo, X.; Liu, F.; Huo, L.; Chen, Y.; Russell, T. P.; Han, C. C.; Li, Y.; Hou, J. *Adv. Mater.* **2012**, *24*, 3383.
- (a) Roncali, J. *Chem. Rev.* **1997**, *97*, 173. (b) Beaujuge, P. M.; Fréchet, J. M. J. *J. Am. Chem. Soc.* **2011**, *133*, 20009. (c) Zhou, H. X.; Yang, L. Q.; You, W. *Macromolecules* **2012**, *45*, 607. (c) Cheng, Y.-J.; Yang, S.-H.; Hsu, C.-S. *Chem. Rev.* **2009**, *109*, 5868.
- (a) Chochos, C. L.; Chouliis, S. A. *Prog. Polym. Sci.* **2011**, *36*, 1326. (b) Huo, L. J.; Hou, J. H. *Polym. Chem.* **2011**, *2*, 2453. (c) Huo, L. J.; Hou, J. H.; Zhang, S. Q.; Chen, H.-Y.; Yang, Y. *Angew. Chem., Int. Ed.* **2010**, *49*, 1500. (d) Huo, L. J.; Guo, X.; Zhang, S. Q.; Li, Y. F.; Hou, J. H. *Macromolecules* **2011**, *44*, 4035.
- (a) Bunz, U. H. F. *Angew. Chem., Int. Ed.* **2010**, *49*, 5037.
- (b) Gidron, O.; Diskin-Posner, Y.; Bendikov, M. *J. Am. Chem. Soc.* **2010**, *132*, 2148.
- (c) Gidron, O.; Dadvand, A.; Sheynin, Y.; Bendikov, M.; Perepichka, D. F. *Chem. Commun.* **2011**, *47*, 1976.
- (d) Woo, C. H.; Beaujuge, P. M.; Holcombe, T. W.; Lee, O. P.; Fréchet, J. M. J. *J. Am. Chem. Soc.* **2010**, *132*, 15547. (e) Bijleveld, J. C.; Karsten, B. P.; Mathijssen, S. G. J.; Wienk, M. M.; Leeuw, D. M.; Janssen, R. A. J. *J. Mater. Chem.* **2011**, *21*, 1600–1606. (f) Li, H.; Jiang, P.; Yi, C.; Li, C.; Liu, S.-X.; Tan, S.; Zhao, B.; Braun, J. R.; Meier, W.; Wandlowski, T.; Decurtins, S. *Macromolecules* **2010**, *43*, 8058.
- (g) Huo, L.; Huang, Y.; Fan, B.; Guo, X.; Jing, Y.; Zhang, M.; Li, Y.; Hou, J. *Chem. Commun.* **2012**, *48*, 3318.
- (h) Coffin, R. C.; Peet, J.; Rogers, J.; Bazan, G. C. *Nat. Chem.* **2009**, *1*, 657.
- (i) Peet, J.; Kim, J. Y.; Coates, N. E.; Ma, W. L.; Moses, D.; Heeger, A. J.; Bazan, G. C. *Nat. Mater.* **2007**, *6*, 497.
- (j) Amb, C. M.; Chen, S.; Graham, K. R.; Subbiah, J.; Small, C. E.; So, F.; Reynolds, J. R. *J. Am. Chem. Soc.* **2011**, *133*, 10062.
- (k) Gunes, S.; Neugebauer, H.; Sariciftci, N. S. *Chem. Rev.* **2007**, *107*, 1324.